Journal of Photochemistry and Photobiology 15 (2023) 100180

Contents lists available at ScienceDirect

Journal of Photochemistry and Photobiology

journal homepage: www.sciencedirect.com/journal/journal-of-photochemistry-and-photobiology

The UV Index color palette revisited

Eduardo Luccini [a,b,*], Facundo Orte [c,d], Julián Lell [e,f], Fernando Nollas [e], Gerardo Carbajal [e], Elián Wolfram [c,e,g]

[a] Consejo Nacional de Investigaciones Científicas y Técnicas (CONICET), Centro de Excelencia en Productos y Procesos de Córdoba (CEPROCOR). Sede Santa María de Punilla, Pabellón Ceprocor (X5164), Córdoba, Argentina
[b] Pontificia Universidad Católica Argentina, Facultad de Química e Ingeniería del Rosario. Av. Pellegrini 3314 (2000), Rosario, Santa Fe, Argentina
[c] Consejo Nacional de Investigaciones Científicas y Técnicas (CONICET). Godoy Cruz 2290 (C1425FQB), Ciudad Autónoma de Buenos Aires, Argentina
[d] Instituto de Investigaciones Científicas y Técnicas para la Defensa, UNIDEF (CITEDEF-CONICET). San Juan Bautista de La Salle 4397 (B1603ALO), Villa Martelli, Buenos Aires, Argentina
[e] Servicio Meteorológico Nacional, Av. Dorrego 4019 (C1425GBE), Ciudad Autónoma de Buenos Aires, Argentina
[f] Universidad Nacional de Luján, Ruta 5 y Avenida Constitución (6700), Luján, Buenos Aires, Argentina
[g] Universidad Tecnológica Nacional, Facultad Regional Buenos Aires, Medrano 951 (C1179AAQ), Ciudad Autónoma de Buenos Aires, Argentina

ARTICLE INFO

Keywords:
UV Index
Color palettes
Color codes
Risk scale
Solar radiation
Public health

ABSTRACT

The UV Index (UVI), standardized by the World Health Organization (WHO) in 2002, is an internationally accepted reference for disseminating information on solar UV radiation levels with the purpose of preventing the harmful effects on human health by sun overexposure. The UVI is the erythemal irradiance expressed in a dimensionless unit, with numerical values adapted to a risk scale that considers the "Extreme" level from a UVI value equal to 11 upwards. This scale is linked to a color palette by health risk ranges, and to a graded color palette by units of UVI for more details. Both the numerical scale and its associated risk levels were universally adopted by the scientific community and by global information systems to the population. However, inconsistencies and limitations persist between both UVI color palettes, making their interpretation and application difficult. In the present work all these aspects are addressed, proposing a revised color palette for unit UVI values that resolves each of them. Based on the WHO risk-ranges UVI color palette, the new color palette for unit UVI values gives coherence to both color charts, allowing reliable identification of the risk level bands and of each unit UVI level within them, and solves the need to distinguish between units for numerical values of UVI higher than 11 that are registered daily in many regions of the world.

1. Introduction

Excessive exposure to solar UV radiation has negative incidence on living organisms (e.g., [8,15,44]). In humans, these include principally damage to the skin, eyes, and immunological system (e.g., [1]). The main consequence of the stratospheric ozone depletion registered in our planet in the last decades is a potential increase of the solar UV radiation levels reaching the Earth's surface, a situation that may get worse by synergistic effects with the current global climate change that overwhelms the Earth's environment (e.g., [4,60]). These processes of anthropic origin, added to some human esthetical-cultural patterns that overvalue the skin suntanning, transform the exposure to solar UV radiation in a critical public health issue (e.g., [39]). On the other hand, the exposure to solar UV radiation in appropriate doses yields positive effects on human health. An updated review on the effects of solar UV radiation exposure on human health was recently presented by Neale et al. [46]. The need to equilibrate harmful with beneficial consequences of solar UV exposure (e.g., [53]) requires that education and disclosure of information to the public be clear and reliable.

The erythemal UV irradiance is the wavelength-integrated UV spectral irradiance weighted by the ISO/CIE [26] action spectrum [54]. The UV Index (UVI) represents the erythemal UV irradiance in a dimensionless unit, obtained as the erythemal UV irradiance in W/m^2 multiplied by a factor of 40 m^2/W. The World Health Organization standardized the UVI in 2002 [55] within the framework of the WHO global Intersun UV project (https://www.who.int/initiatives/intersun-program), becoming

* Corresponding author at: CONICET - Centro de Excelencia en Productos y Procesos de Córdoba (CEPROCOR). Sede Santa María de Punilla, Pabellón Ceprocor (X5164), Córdoba, Argentina.
E-mail address: eluccini@ceprocor.uncor.edu (E. Luccini).

https://doi.org/10.1016/j.jpap.2023.100180

Available online 27 April 2023

Table 1
UVI color palette by risk ranges [55].

Risk level	Numerical UVI value(1)	Color code					
		PMS	Hex/HTML	RGB	CMYK	HSL	HSV
Low	0 ≤ UVI < 3	375 C	#97D700	151,215,0	30%, 0%, 100%, 16%	78°, 100.0%, 42.2%	78°, 100.0%, 84.3%
Moderate	3 ≤ UVI < 6	102 C	#FCE300	252,227,0	0%, 10%, 100%, 1%	54°, 100.0%, 49.4%	54°, 100.0%, 98.8%
High	6 ≤ UVI < 8	151 C	#FF8200	255,130,0	0%, 49%, 100%, 0%	31°, 100.0%, 50.0%	31°, 100.0%, 100.0%
Very High	8 ≤ UVI < 11	032 C	#EF3340	239,51,64	0%, 79%, 73%, 6%	356°, 85.5%, 56.9%	356°, 78.7%, 93.7%
Extreme	UVI ≥ 11	265 C	#9063CD	144,99,205	30%, 52%, 0%, 20%	265°, 51.5%, 59.6%	265°, 51.7%, 80.4%

(1) The validity limits of each range are explicitly expressed, emphasizing the real-number character of the UVI values.

an international reference tool for evaluating the risks to humans under excessive exposure to solar radiation, used for wide dissemination of public information to prevent massive health damage. UVI values are disaggregated into a numerical scale by ranges of health risk, with identifying color and protecting recommendations associated to each range. The WHO [55] document recommends expressing the UVI as entire numbers, using some rounding criteria. Thus, green color is assigned for UVI < 2 ("Low" risk), yellow color for UVI $= 3$ to 5 ("Moderate" risk), orange color for UVI $= 6$ to 7 ("High" risk), red color for UVI $= 8$ to 10 ("Very High" risk), and violet color for UVI ≥ 11 ("Extreme" risk), constituting the WHO [55] risk-ranges UVI color palette. Additionally, the WHO [55] document recommends implementing a detailed graded color palette by units of UVI to distinguish between intermediate integer values, providing in its Annex D a color palette for unit UVI values that for UVI ≥ 11 is also completed with a single violet color. An attached graphics package to the WHO [55] document promotes standards for the presentation of the UVI including the UVI logo, icons for UVI reporting, sun protection icons, and color codes for different values of the UVI [57].

Recent studies evaluated the UVI information performance since the WHO [55] standardization, outlining strengths but also limitations in their understanding, use and divulgation (e.g., [3,14,16,22,27,32,33]). Permanent developments deploy new tools for disseminating public UVI information, as the SunSmart Global UV App for mobile phones launched in June 2022 [56]. Revision by official commissions detected no need for significant changes neither in the numerical UVI risk scale nor in the UVI policies [2,18]. The last reported official remarks on UVI guidelines were made during the Intersun Programme's 7th International Advisory Committee Meeting [25]. Nevertheless, the sharp identification of UVI levels through colors on plots and maps using the defined WHO [55] UVI color palettes still presents difficulties due to inconsistencies that require a rethinking. Particularly in the "Extreme" risk level, factors such as altitude, latitude, surface albedo, some types of clouds, depleted stratospheric ozone content mainly in polar regions and mini-ozone holes, among others, cause that many regions in the world register UVI largely above 11, reaching values of 20 or more during spring-summer along wide areas of the planet such as the South American Andean Altiplano, the Tibetan Plateau, the Australian Desert and the inter-tropical planetary region in general (e.g., [7,10,12,17,31,34,36,37,40]). Color issues using the WHO [55] convention were first pointed out by Liley and McKenzie [35], expanded later in recommendations by Zaratti et al. [62]. Some attempts to distinguish between UVI values higher than 11 with colors had a merely demonstrative character and were not linked to the WHO [55] palette (e.g., [13,34,45,47]). Other practical example is given by the TEMIS/ESA (Tropospheric Emission Monitoring Internet Service), whose world UVI data (https://www.temis.nl/uvradiation/UVindex.php) are deployed in an alternative default color map to show a wider range of variability than allowed by the WHO [55] palette for UVI values ≥ 11.

UVI maps show strong regional gradients caused primarily by surface elevation and albedo in the clear-sky case, while clouds impinge significant additional gradients. In turn, measurements and calculations of solar UVI are often presented over the background of the defined UVI color palette to emphasize the relation of UVI values with health risk. Then, counting with an adequate color palette for unit UVI values is crucial to distinguish the UVI at all geographic scales and in the whole range of possible UVI registers. Taking the WHO [55] risk-ranges UVI color palette as a reference, the color palette for unit UVI values (UCP_{UVI}) is wholly revisited in this work. A revised UCP_{UVI} is proposed that solves each detected inconsistency, to be considered for its implementation as an updated version of the recommended WHO [55] UCP_{UVI}.

2. Generation of the new color palette for unit UVI values

As the WHO [55] document specifies, the choice of colors in the risk-ranges UVI color palette was not made on a scientific basis, although it responds to the color wheel structure firstly defined by Newton [48] and the color risk identification can be associated presently to the "traffic light logic". Given that the UVI is a dimensionless expression of the erythemal UV irradiance, then a real number not rounded in many applications, the UVI limit values for each range are explicitly detailed from now on. So, green color is assigned to $0 \leq$ UVI < 3 ("Low" risk), yellow color to $3 \leq$ UVI < 6 ("Moderate" risk), orange color to $6 \leq$ UVI < 8 ("High" risk), red color to $8 \leq$ UVI < 11 ("Very High" risk), and violet color to UVI ≥ 11 ("Extreme" risk). In the WHO [55] document the reference colors for the risk-ranges UVI color palette are given in Pantone Matching System (PMS) color code. At present, the most used Pantone code in graphic design applications is PMS "C" for printing on coated paper, and its use can be considered an update that this work proposes. For greater detail, Table 1 presents the risk-ranges

Table 2
Proposed unit UVI color palette (left) and WHO [55] unit UVI color palette (right).

Proposed UCP_{UVI}

Risk level[1]	Numerical UVI value[2]	Color code[3] PMS	Color code[3] Hex
Low	0 ≤ UVI < 1	370 C	#658D1B
	1 ≤ UVI < 2	376 C	#84BD00
	2 ≤ UVI < 3	375 C	#97D700
Moderate	3 ≤ UVI < 4	101 C	#F7EA48
	4 ≤ UVI < 5	102 C	#FCE300
	5 ≤ UVI < 6	116 C	#FFCD00
High	6 ≤ UVI < 7	157 C	#ECA154
	7 ≤ UVI < 8	151 C	#FF8200
Very High	8 ≤ UVI < 9	032 C	#EF3340
	9 ≤ UVI < 10	485 C	#DA291C
	10 ≤ UVI < 11	193 C	#BF0D3E
Extreme	11 ≤ UVI < 12	265 C (d27%)	#4B1E88
	12 ≤ UVI < 13	265 C (d18%)	#62359F
	13 ≤ UVI < 14	265 C (d9%)	#794CB6
	14 ≤ UVI < 15	265 C	#9063CD
	15 ≤ UVI < 16	265 C (l9%)	#A77AE4
	16 ≤ UVI < 17	265 C (l18%)	#BE91FB
	17 ≤ UVI < 18	265 C (l27%)	#D5A8FF
	18 ≤ UVI < 19	265 C (l36%)	#ECBFFF
	19 ≤ UVI < 20	265 C (l45%)	#FFD6FF
	20 ≤ UVI < 21	265 C (l54%)	#FFEDFF
	UVI ≥ 21	White	#FFFFFF

(1) The colors in this column correspond to the reference risk-ranges UVI color palette (Table 1).
(2) The validity limits of each range are explicitly expressed, emphasizing the real number character of the UVI values.
(3) Violet tones in the "Extreme" risk level were obtained by darkening (d) or lightening (l) the PMS 265 C color in the indicated percentage.

WHO [55] UCP_{UVI}

Risk level[1]	Numerical UVI value[2]	Color code[2] Hex
Low	0 to 2	#4EB400
	2 to 3	#A0CE00
Moderate	3 to 4	#F7E400
	4 to 5	#F8B600
	5 to 6	#F88700
High	6 to 7	#F85900
	7 to 8	#E82C0E
Very High	8 to 9	#D8001D
	9 to 10	#FF0099
	10 to 11	#B54CFF
Extreme	11 or more	#998CFF

(1) The colors in this column correspond to the reference risk-ranges UVI color palette (Table 1).
(2) As defined in the WHO [55] document.

UVI color palette in force using the WHO [55] PMS numbers now in PMS "C" code, as well as in other commonly used codes: Hexadecimal or Hyper Text Markup Language (Hex/HTML), Red, Green, Blue 24-bit (RGB), Cyan, Magenta, Yellow, Black (CMYK), Hue, Saturation, Lightness (HSL), and Hue, Saturation, Value (HSV). This risk-ranges UVI color palette constitutes the basis for the development of the revised UCP_{UVI} proposed in this work.

2.1. Criteria to generate the new color palette for unit UVI values

The palette of colors for unit UVI values presented in the Annex D of the WHO [55] document contrasts and presents inconsistencies with the risk-ranges UVI color palette that the same document standardizes (as an example, even the single violet color that identifies the "Extreme" risk range is different in both WHO [55] palettes). Then, a revised color palette for unit UVI values was developed, according to the following criteria:

- The new UCP_{UVI} must be based on the standard risk-ranges UVI color palette [55], i.e., the color tones of the new UCP_{UVI} must obey, within each risk level, the color structure of Table 1. To achieve this more rigorously, each color in the risk-ranges UVI color palette (Table 1) must be part of the new UCP_{UVI}, constituting a unit UVI tone within its corresponding risk-range color.
- When applied to maps and graphs, the new UCP_{UVI} must primarily allow identifying the color bands by risk ranges, to later differentiate in greater detail (if necessary, with sufficient magnification) the tones within each color for unit UVI values. A clear visualization must be achieved both on screen in different devices and printed in different types of paper.
- As in the presentation of the risk-ranges UVI color palette in Table 1, each color tone in the new UCP_{UVI} must be identified in the principal commonly used color codes, particularly in PMS given the multiple applications of PMS-coded colors, although the significantly smaller number of available tones in the PMS C code (approximately 15,000) constraints the selection compared to those provided by RGB 24-bit (more than 16,000,000).
- The new UCP_{UVI} must allow distinguishing between unit values for UVI $\geq$ 11 in maps and graphs. This solution must be obtained from the violet color that defines the "Extreme" range in the risk-ranges UVI color palette (Table 1).

Following the procedure detailed in Appendix A, the proposed UCP_{UVI} was determined according to the aforementioned guidelines. It is shown in Table 2-left, together with the WHO [55] UCP_{UVI} (Table 2-right) for comparison. Even though the new palette could not be elaborated on the base of rigorous technical algorithms (e.g., [23,29,30,43,50,58,61]) nor perceptual criteria (e.g., [5,9,11,19,20,28,52,59]), a basic colorimetric analysis, shown in Appendix B, provides technical support to the proposed UCP_{UVI}. The following section details the inconsistencies detected in the WHO [55] UCP_{UVI}, and the solution that the new UCP_{UVI} supplies to each of them.

3. Detected inconsistencies and proposed solutions

This section details the inconsistencies detected in the WHO [55] UCP_{UVI} (Table 2-right), as well as the solution provided by the proposed UCP_{UVI} (Table 2-left) to each of them.

3.1. Coherence between the UCP_{UVI} and the risk-ranges UVI color palette

The WHO [55] UCP_{UVI} (Table 2-right) presents several tones that do not correspond with the risk-ranges UVI color palette (Table 1), such as orange tones in the "Moderate" range, a tone of red color in the "High" range, a tone of violet color in the "Very High" range and, as mentioned, the single violet color that identifies the "Extreme" risk range is different in both WHO [55] palettes. On the other hand, Table 2-right does not present any tone extracted from Table 1, resulting in a disconnection between the UCP_{UVI} and the risk-ranges UVI color palette. Both aspects are resolved in the proposed UCP_{UVI} (Table 2-left), since it consists exclusively of tones of the corresponding color in each risk range: green for "Low" risk, yellow for "Moderate" risk, orange for "High" risk, red for "Very High" risk, and violet for "Extreme" risk. As an additional link, the new UCP_{UVI} incorporates the colors from Table 1 as one of the tones in its corresponding risk range.

3.2. Distinction between UVI values in the range 0 to 2

In the WHO [55] UCP_{UVI} (Table 2-right) the UVI levels between 0 and 1, and between 1 and 2 are indistinguishable, both under the same tone of green. This is solved in the proposed UCP_{UVI} (Table 2-left) with three different tones of green for UVI between 0 and 1, between 1 and 2 and between 2 and 3 within the "Low" risk level, one of whose tones ($2 \leq$ UVI < 3) is now the PMS 375 C from Table 1. This is a crucial improvement, given recent calls for attention to flawed protection messages that do not take exposure time into account, especially for UVI < 3 (e.g., [38,41]). Official UVI remarks [25] took these concerns, that long exposure times can still lead to harm health effects even in the "Low" risk range, when the balance with beneficial effects of solar UV exposure becomes critical.

3.3. Extension of the limit to distinguish unit UVI values up to 21+

The proposed UCP_{UVI} (Table 2-left) contains a gradient of tones that become lighter as the UVI increases in the "Extreme" risk range, allowing the distinction between unit UVI values higher than 11 that daily occur in large regions of the world. It was elaborated on the base of the PMS 265 C violet color that defines the "Extreme" range in Table 1, assigned in the proposed UCP_{UVI} to $14 \leq$ UVI < 15, with systematic lightening (darkening) in steps of 9% for smaller (greater) values until the white color that is reached for UVI of 21 or higher. The threshold value of 21 to distinguish tones in the new UCP_{UVI} is considered appropriate for two key aspects: as an easily identifiable number with respect to the UVI value of 11 at which the "Extreme" risk level begins, and as a threshold representative of the maximum UVI values that are often registered throughout the world.

3.4. Clarification of the boundaries between each unit and each risk level

Even when the disclosure of the UVI to the public is typically done in the form of integer numbers under some rounding criteria [55], it must always be borne in mind that at all situations (measurements, calculations, graphs, maps, etc.) the UVI represents a real number that expresses the erythemal UV irradiance in a dimensionless unit. To properly identify which risk level and color a given UVI value corresponds to, the limits between UVI intervals must be explicitly established in both palettes, as now in Table 1 and Table 2-left.

3.5. Palette supplied in the most used color codes

To establish a precise and unambiguous standard, the UCP_{UVI} proposed in Table 2-left is detailed in Appendix C in the same set of commonly used color codes than the risk-ranges UVI color palette shown in Table 1.

4. Applications

Fig. 1 shows the proposed UCP_{UVI} (Fig. 1-left) and the WHO [55] risk-ranges UVI color palette (Fig. 1-right) as a background for UVI measurements at the tropical high-altitude La Quiaca station (22.11°S, 65.57°W, 3459 m a.s.l.) in the Argentine Andean Plateau [10]. Data were recorded every 1 min with a traceably calibrated sensor [49]

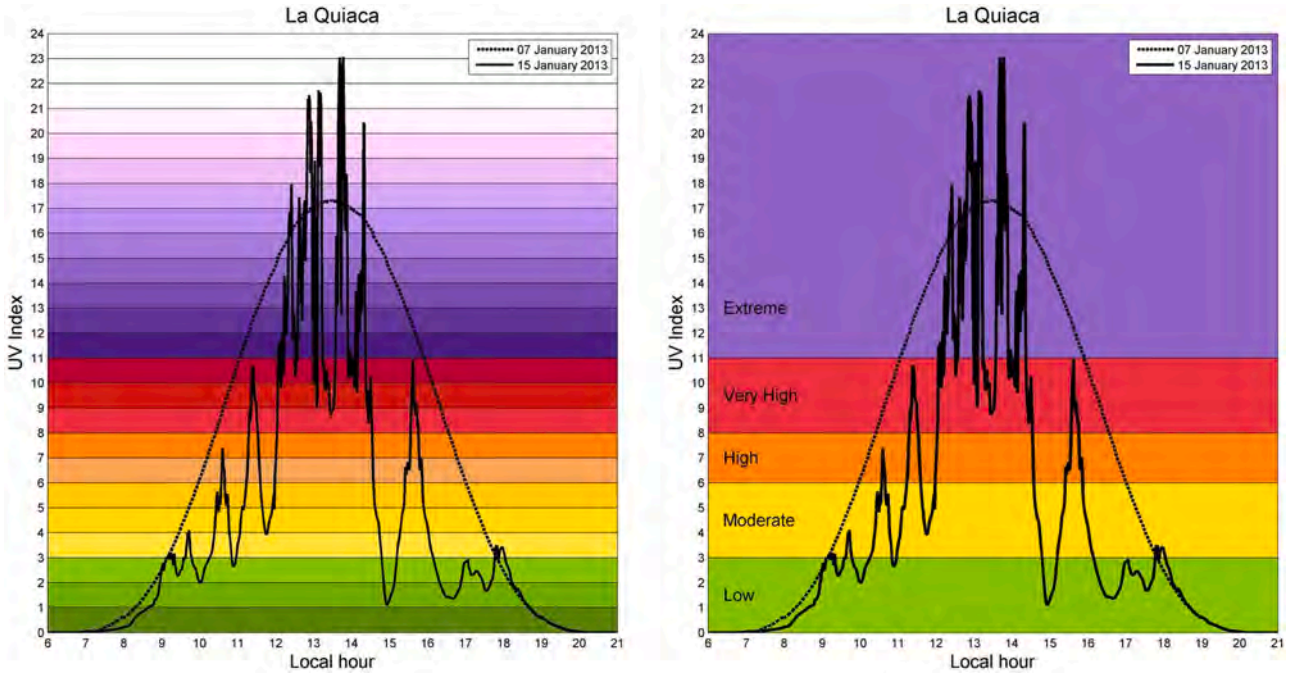

Fig. 1. Application of the proposed new UCP_{UVI} (left) and of the standard color palette by risk ranges [55] (right) to UVI measurements recorded every 1 min during 07 January 2013 (under clear-sky conditions) and 15 January 2013 (with scattered clouds) at La Quiaca station (22.11°S, 65.57°W, 3459 m a.s.l.) of the Argentine UV Monitoring Network.

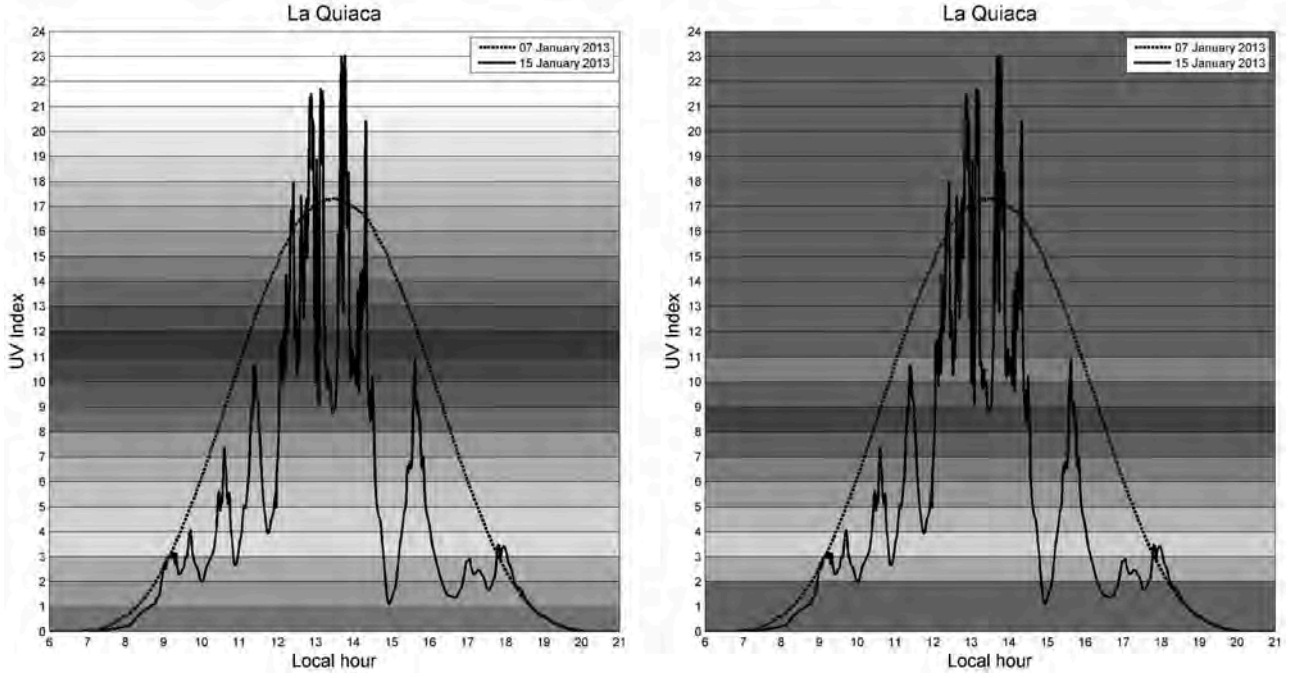

Fig. 2. (left) Conversion to luminance of the new UCP_{UVI} from Fig. 1-left, and (right) luminance of the WHO [55] UCP_{UVI}.

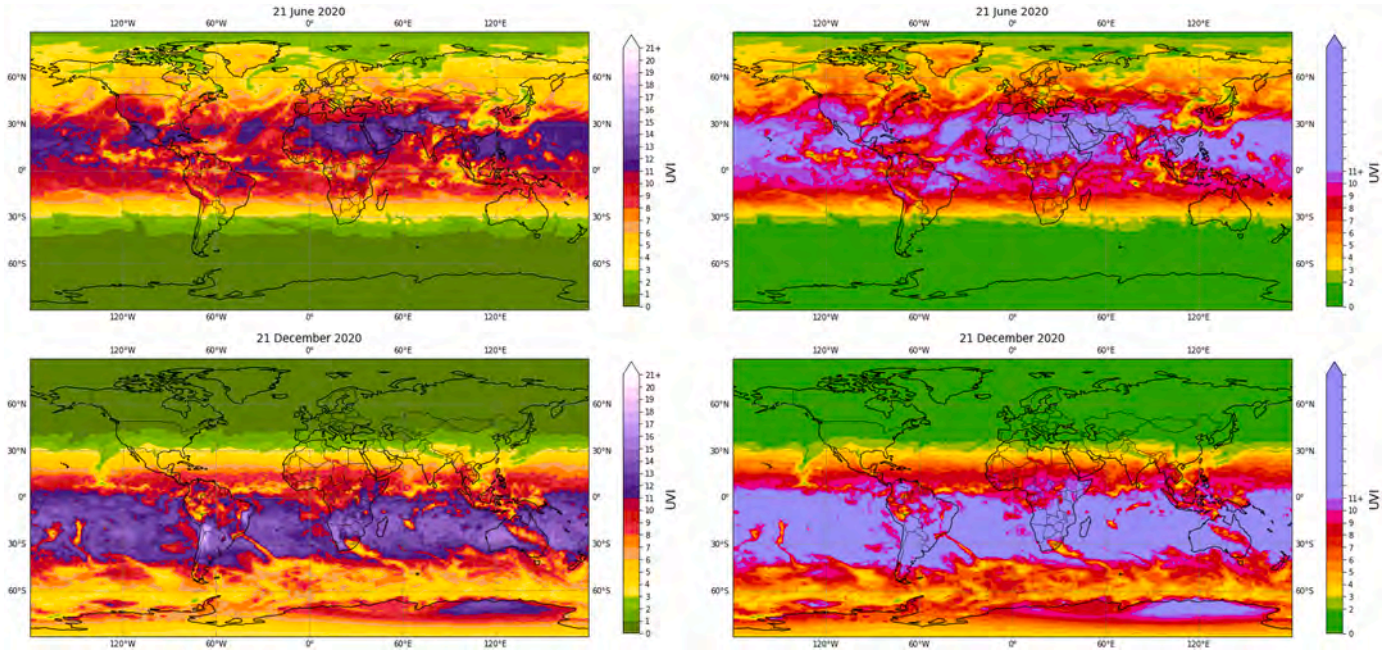

Fig. 3. Application of the proposed UCP_{UVI} (left) and comparison with the WHO [55] UCP_{UVI} (right) to noon all-sky daily global UVI data provided by CERES (https://ceres.larc.nasa.gov/index.php) for 21 June 2020 (top) and 21 December 2020 (bottom).

during two days of January 2013. UVI values over 17 can be registered during a clear-sky day close to the summer solstice (07 January 2013). Meanwhile, under certain conditions including the presence of scattered cumulus clouds around the sun's position, UV radiation can be intensified for several minutes up to UVI values higher than 23 as measured on 15 January 2013. The proposed UCP_{UVI} (Fig. 1-left) exhibits full coherence with the risk-ranges UVI color palette (Fig. 1-right), allowing firstly to identify the color bands corresponding to each health risk interval, and next a clear distinction between unit UVI values even in the "Extreme" risk range.

According to the development guidelines detailed in Appendix A, and the luminance analysis explained in Appendix B, Fig. 2-left presents the conversion to luminance of Fig. 1-left where the proposed UCP_{UVI} is applied, showing smooth alternate luminance gradients that would allow still a clear identification of unit UVI levels in grayscale plots and maps. On the other hand, Fig. 2-right, that shows the conversion to luminance of the WHO [55] UCP_{UVI}, presents an irregular alternation of high and low luminance levels and a homogeneous luminance for UVI $\geq$ 11, that seriously limit the capability of discerning between unit UVI values in grayscale plots and maps.

Fig. 3 shows the global maps of noon all-sky UVI data retrieved by CERES (Clouds and the Earth's Radiant Energy System) [51] during days close to the solstices of year 2020, 21 June (Fig. 3-top) and 21 December (Fig. 3-bottom). The advantages that the new UCP_{UVI} (Fig. 3-left) offers to observe regional features in the UVI values are evident compared to the WHO [55] UCP_{UVI} (Fig. 3-right). In Appendix D, these advantages are emphasized on regional zooms within the global maps of Fig. 3, and on an example of ozone hole event over Antarctica and its surroundings.

5. Discussion and conclusions

Based on the standard UVI color palette by risk ranges [55], a comprehensive proposal has been presented to improve their associated color palette that allows distinguish details by UVI units. It corrects detected inconsistencies and extends the possibility of discerning in plots and maps between unit UVI values greater than 11, daily recorded in large regions of the world in the "Extreme" health risk range. Considering that the current WHO UVI convention has been used by the scientific and by the global public communities for more than 20 years, the WHO [55] standardized color structure of the palette by risk ranges could remain unalterable. According to this premise, the elaboration of the proposed color palette for unit UVI values is based on it. Nevertheless, if a major revision were considered appropriate it was noted, within the different tested alternatives, that a gradient of burgundy (e.g., PMS 187 C) or purple (e.g., PMS 246 C) tones for the 11+ "Extreme" risk range could give even better results in both aspects: the continuity of the red colors from the "Very High" risk level and to improve the visual identification of unit UVI values over 11.

Unlike the current situation, where the application of innumerable locally defined ad-hoc color palettes leads to confusion in interpreting and comparing UVI graphic information, the implementation of the proposed color palette for unit values of the UV Index as a new international standard, or an eventual alternative that similarly overcomes the detected inconsistencies, would imply significant improvements. The availability of both coherent UV Index color palettes, by risk ranges and for unit UVI values, would promote the use of uniform standards by the scientific community to present and analyze their research results, and by the national weather agencies that daily publish the UV Index forecast and information. Consequently, this would boost its general use by all other official and private UVI information systems, achieving

more efficiently the purpose of the UVI as crucial public health care tool to prevent excessive unprotected exposure to the sun. Revisions carried out by WHO-convened official commissions that periodically evaluate the UV Index guidelines and performance, such as the cited from 2011 to 2015 UVI working group workshops, are the appropriate environment to gather and promote the proposals towards the approval of new standards. Given that the latest official remarks on UVI guidelines date back to the year 2018, a prompt approach to these issues, taking a new step towards even better UVI standards, would be highly recommended.

Funding

This work was supported by the Argentine National Agency for the Promotion of Research, Technological Development and Innovation, within the framework of project code PICT-2020-SERIEA-02601.

CRediT authorship contribution statement

Eduardo Luccini: Conceptualization, Methodology, Software, Validation, Formal analysis, Writing – original draft, Writing – review & editing, Visualization, Supervision, Project administration, Funding acquisition. **Facundo Orte:** Software, Validation, Data curation, Visualization, Writing – review & editing, Funding acquisition. **Julián Lell:** Software, Validation, Visualization, Writing – review & editing. **Fernando Nollas:** Data curation, Writing – review & editing. **Gerardo Carbajal:** Writing – review & editing, Funding acquisition. **Elián Wolfram:** Writing – review & editing, Funding acquisition.

Declaration of Competing Interest

The authors declare that they have no known competing financial interests or personal relationships that could have appeared to influence the work reported in this paper.

Data availability

Data will be made available on request.

Acknowledgements

The authors acknowledge the personnel from La Quiaca station of the Argentine UV Monitoring Network, and to the participating institutions for the facilities and encouragement to develop this work. A special thanks to two anonymous reviewers, whose comments and suggestions contributed to the improvement of the manuscript. Global UVI data were provided by CERES (Clouds and the Earth's Radiant Energy System, https://ceres.larc.nasa.gov/index.php).

Appendix A

Procedure to generate the new UCP_{UVI}

Since color perception depends on a huge variety of conditions, including those inherent to the observers themselves (e.g., [21]), the definition of a revised standard UCP_{UVI} intended for millions of people around the world requires an objective methodology, to select the color tones on technical aspects. In the RGB code, a tone obtained by darkening or lightening of a given color is defined by the following equation:

$$\overrightarrow{C_T} = \overrightarrow{C_O} \pm 255 * F * \overrightarrow{C_1} \quad \text{(eA1)}$$

Where $\overrightarrow{C_T}$ and $\overrightarrow{C_O}$ are the "color vectors" in the RGB space whose components are the integer numbers that represent each RGB component (in the range [0–255]), for the obtained tone ($\overrightarrow{C_T}$, defined under some rounding criteria if necessary) and for the original color ($\overrightarrow{C_O}$). $\overrightarrow{C_1}$ is the color vector with components (1,1,1) and F is the fraction of darkening (applying the "-" sign in equation eA1) or lightening (applying the "+" sign in equation eA1) with respect to the original color. For example, F equals 0.15 for a 15% darkening or lightening. Truncation is applied at 0 or 255 in case that any of the RGB components of $\overrightarrow{C_T}$ exceeds these limits when applying equation (eA1) for the generation of the different tones.

Then, based on the criteria detailed in Section 2.1, the proposed UCP_{UVI} was established according to the following stages:

1) An appropriate assignment of each color in Table 1 to an appropriate UVI level in the new UCP_{UVI} was sought, according to its tone. Thus, PMS 375 C was assigned to the unit range $2 \leq UVI < 3$, PMS 102 C to $4 \leq UVI < 5$, PMS 151 C to $7 \leq UVI < 8$, PMS 032 C to $8 \leq UVI < 9$ and PMS 265 C to $14 \leq UVI < 15$.
2) Preliminary color tones in RGB 24-bit code were established for unit UVI values within each risk range from Table 1 in the interval $0 \leq UVI < 11$, based on the darkening or lightening in 10% steps of the corresponding color in Table 1, using equation (eA1). From these, a basic unit UVI RGB palette was selected, allowing a clear visualization under a wide variety of tests: on different types of screens (PCs, notebooks, cell phones and tablets), under different conditions of brightness and contrast, varying the viewing angle of the user regarding the screen, as well as printing tests both in color and in grayscale on different types of paper.
3) Once these basic unit UVI tones in the range $0 \leq UVI < 11$ were defined in RGB code, the closest colors to each of them in PMS C code were identified and selected.
4) When several PMS C tones of a given color seemed appropriate for a unit UVI level, the selection was guided by the luminance gradient criteria (see Appendix B) to make each tone distinguishable from its immediate neighbors also in grayscale.
5) Finally, for $UVI \geq 11$, darkening and lightening tests using equation (eA1) were carried out in different percentages from the PMS 265 C color (Table 1) to generate the tones of violet color that allow discernment between unit UVI values in the "Extreme" risk level. A gradient in systematic percentages of 9% was found appropriate, with the white color characterizing uniformly the range $UVI \geq 21$.

Appendix B

Basic colorimetric analysis of the proposed UCP_{UVI}

As detailed in Section 2, the determination of tones for the new UCP_{UVI} (Table 2-left) was based on the colors of the standard WHO [55] risk-ranges UVI color palette (Table 1), prioritizing tones that are identifiable in the most widely used color codes, including PMS C which has fewer available options. Once established the new UCP_{UVI}, it is important to rank the choice by verifying that certain colorimetric analysis criteria are met. A guideline to verify is that two colors are clearly distinguishable (by people without alterations in visual perception) if they are far enough apart in the 3D RGB space. The procedure to establish the revised UCP_{UVI}, detailed in Appendix A, requests that the "colors" (that is, the set of tones corresponding to each color within the risk-ranges UVI color palette) were appropriately grouped and separated from each other. The 3D RGB graphical representation of Figure B1-left shows that this guideline is accomplished by the new palette. On the contrary, Fig. B1-right demonstrates that in the WHO [55] UCP_{UVI} there is no possible identification of color "groups" consistent with the WHO [55] risk-ranges UVI color palette. Additionally, the appropriate separation between consecutive tones within each color in Figure B1-left is a good indicator of the ability to distinguish each tone from its immediate neighbors in the proposed palette. Likewise, the straight line in the 3D RGB space of Figure B1-left, that represents the progressive lightening of violet tones for UVI values from 11 upwards, is consistent with equation (eA1) with the percentages accounted in Table 2-left, and the departure from the straight line towards the white color is the result of truncation in 255 in equation (eA1).

Other crucial test is the capability of the UCP_{UVI} to distinguish immediate neighbor values even in the grayscale of monochrome (black and white) screens or printers, achieved by performing a transformation to luminance (Y) as defined under the National Television Systems Committee (NTSC) standards [24], according to the equation:

$$Y = (0.30 * R + 0.59 * G + 0.11 * B)/255 \quad \text{(eB1)}$$

where R, G and B take their current values in the range [0–255].

Obviously, an optimal color palette would have a monotonous luminance gradient to infer features and values unambiguously also in grayscale [42]. Even though this is not strictly feasible in our case, where the color selection for the revised UCP_{UVI} is constrained to the standard WHO [55] risk-ranges UVI color palette, a smooth alternation of few luminance gradients across the palette is desirable rather than numerous random luminance jumps.

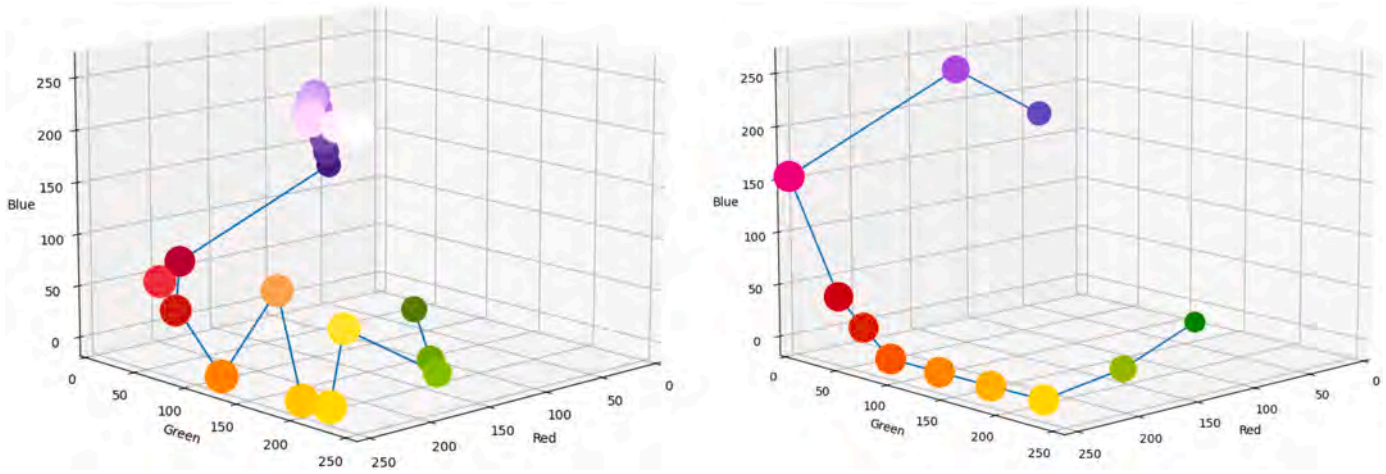

Fig. B1. 3D graphical representation in the RGB space of the proposed UCP_{UVI} (left) and the WHO [55] UCP_{UVI} (right).

Appendix C

Table C1
Proposed new color palette for unit UVI values, in the main standard color codes.

Numerical UVI value	Color code					
	PMS	Hex/HTML	RGB	CMYK	HSL	HSV
0 ≤ UVI < 1	370 C	#658D1B	101,141,27	28%, 0%, 81%, 45%	81°, 67.9%, 32.9%	81°, 80.9%, 55.3%
1 ≤ UVI < 2	376 C	#84BD00	132,189,0	30%, 0%, 100%, 26%	78°, 100.0%, 37.1%	78°, 100.0%, 74.1%
2 ≤ UVI < 3	375 C	#97D700	151,215,0	30%, 0%, 100%, 16%	78°, 100.0%, 42.2%	78°, 100.0%, 84.3%
3 ≤ UVI < 4	101 C	#F7EA48	247,234,72	0%, 5%, 71%, 3%	56°, 91.6%, 62.5%	56°, 70.9%, 96.9%
4 ≤ UVI < 5	102 C	#FCE300	252,227,0	0%, 10%, 100%, 1%	54°, 100.0%, 49.4%	54°, 100.0%, 98.8%
5 ≤ UVI < 6	116 C	#FFCD00	255,205,0	0%, 20%, 100%, 0%	48°, 100.0%, 50.0%	48°, 100.0%, 100.0%
6 ≤ UVI < 7	157 C	#ECA154	236,161,84	0%, 32%, 64%, 7%	30°, 80.0%, 62.7%	30°, 64.4%, 92.5%
7 ≤ UVI < 8	151 C	#FF8200	255,130,0	0%, 49%, 100%, 0%	31°, 100.0%, 50.0%	31°, 100.0%, 100.0%
8 ≤ UVI < 9	032 C	#EF3340	239,51,64	0%, 79%, 73%, 6%	356°, 85.5%, 56.9%	356°, 78.7%, 93.7%
9 ≤ UVI < 10	485 C	#DA291C	218,41,28	0%, 81%, 87%, 15%	4°, 77.2%, 48.2%	4°, 87.2%, 85.5%
10 ≤ UVI < 11	193 C	#BF0D3E	191,13,62	0%, 93%, 68%, 25%	343°, 87.3%, 40.0%	343°, 93.2%, 74.9%
11 ≤ UVI < 12	265 C (d27%)	#4B1E88	75,30,136	45%, 78%, 0%, 47%	265°, 63.9%, 32.5%	265°, 77.9%, 53.3%
12 ≤ UVI < 13	265 C (d18%)	#62359F	98,53,159	38%, 67%, 0%, 38%	265°, 50.0%, 41.6%	265°, 66.7%, 62.4%
13 ≤ UVI < 14	265 C (d9%)	#794CB6	121,76,182	34%, 58%, 0%, 29%	265°, 42.1%, 50.6%	265°, 58.2%, 71.4%
14 ≤ UVI < 15	265 C	#9063CD	144,99,205	30%, 52%, 0%, 20%	265°, 51.5%, 59.6%	265°, 51.7%, 80.4%
15 ≤ UVI < 16	265 C	#A77AE4	167,122,228	27%, 46%,	265°, 66.3%,	265°, 46.5%,

(*continued on next page*)

Table C1 (*continued*)

	(l9%)			0%, 11%	68.6%	89.4%
16 ≤ UVI < 17	265 C (l18%)	#BE91FB	190,145,251	24%, 42%, 0%, 2%	265°, 93.0%, 77.6%	265°, 42.2%, 98.4%
17 ≤ UVI < 18	265 C (l27%)	#D5A8FF	213,168,255	16%, 34%, 0%, 0%	271°, 100.0%, 82.9%	271°, 34.1%, 100.0%
18 ≤ UVI < 19	265 C (l36%)	#ECBFFF	236,191,255	7%, 25%, 0%, 0%	282°, 100.0%, 87.5%	282°, 25.1%, 100.0%
19 ≤ UVI < 20	265 C (l45%)	#FFD6FF	255,214,255	0%, 16%, 0%, 0%	300°, 100.0%, 92.0%	300°, 16.1%, 100.0%
20 ≤ UVI < 21	265 C (l54%)	#FFEDFF	255,237,255	0%, 7%, 0%, 0%	300°, 100.0%, 96.5%	300°, 7.1%, 100.0%
UVI ≥ 21	White	#FFFFFF	255,255,255	0%, 0%, 0%, 0%	0°, 0.0%, 100.0%	0°, 0.0%, 1.0%

Appendix D

Regional details revealed by the proposed UCP_{UVI}

The advantages that the new UCP_{UVI} offers to observe regional features in the UVI values, compared to the WHO [55] UCP_{UVI}, is highlighted in Figs. D1 and D2 that represent geographical zooms on the maps of Fig. 3 for South America (Fig. D1) and for the Tibetan Plateau (Fig. D2), regions with strong UVI gradients and extreme values that widely exceed 11 during great part of the year, emphasizing the reliability of the new UCP_{UVI} (Figures D1-left and D2-left) to distinguish territorial details in both the high spring-summer and the low autumn-winter UVI values. Fig. D3 presents a critical situation where the necessity to observe high-level and high-gradient UVI regional features is crucial, as the case of an Antarctic ozone hole event overpassing continental areas of southern South America and its surroundings like that registered by CERES data on day 01 December 2020. The new UCP_{UVI}, applied in Fig. D3-left, proves to be much more efficient in displaying those details. It is interesting to note that the CERES UVI value determined under noon clear-sky conditions on day 01 December 2020 at the pixel containing Palmer Antarctic station (64.77°S, 64.05°W, 21 m a.s.l.) is 12.6, indeed in the range of maximum historical ground-based measurement registers at this site [6].

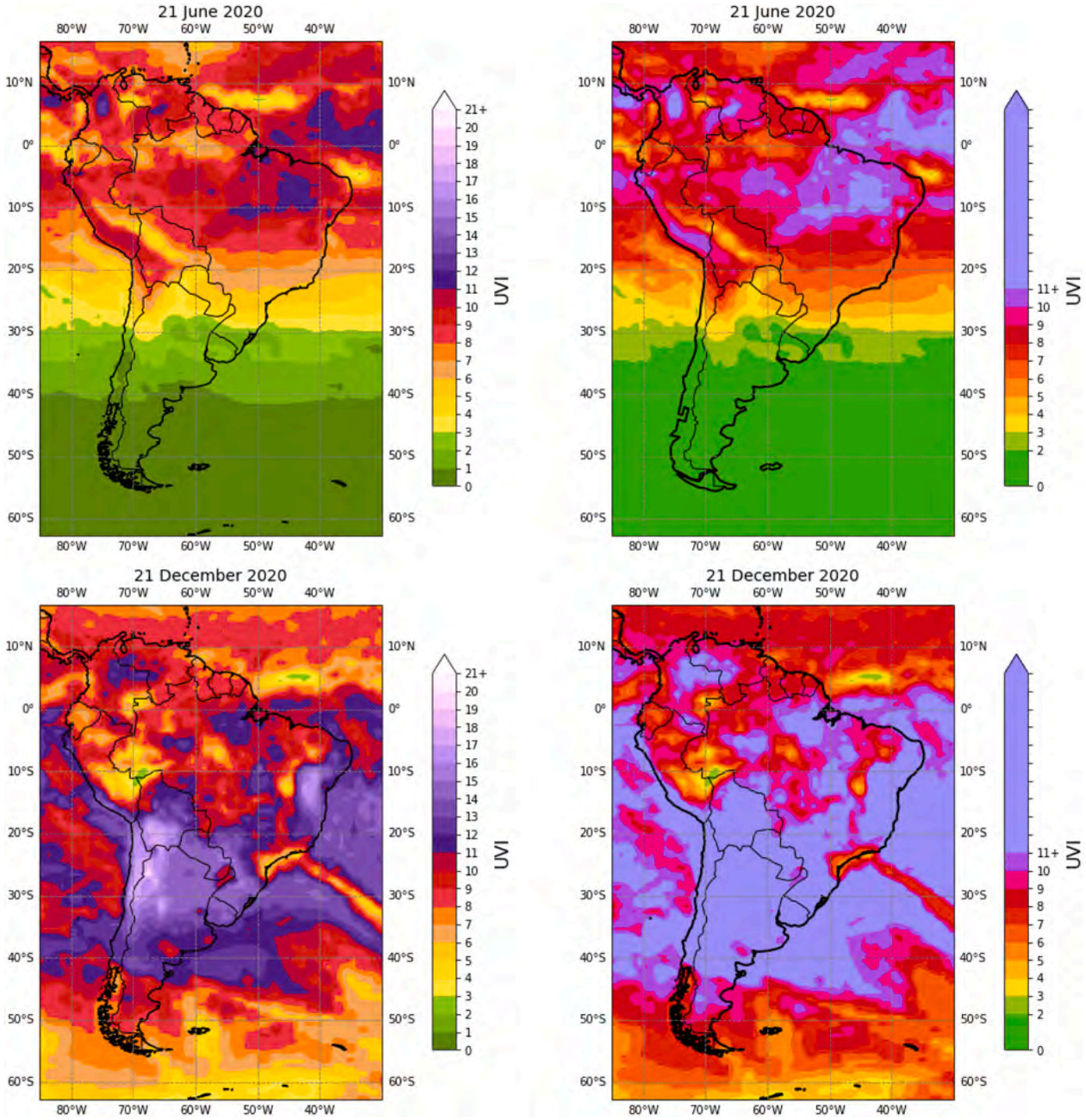

Fig. D1. Application of the proposed UCP_{UVI} (left) and comparison with the WHO [55] UCP_{UVI} (right) to a zoom on the maps of Fig. 3 spanning the territory of South America and its surroundings for 21 June 2020 (top) and 21 December 2020 (bottom).

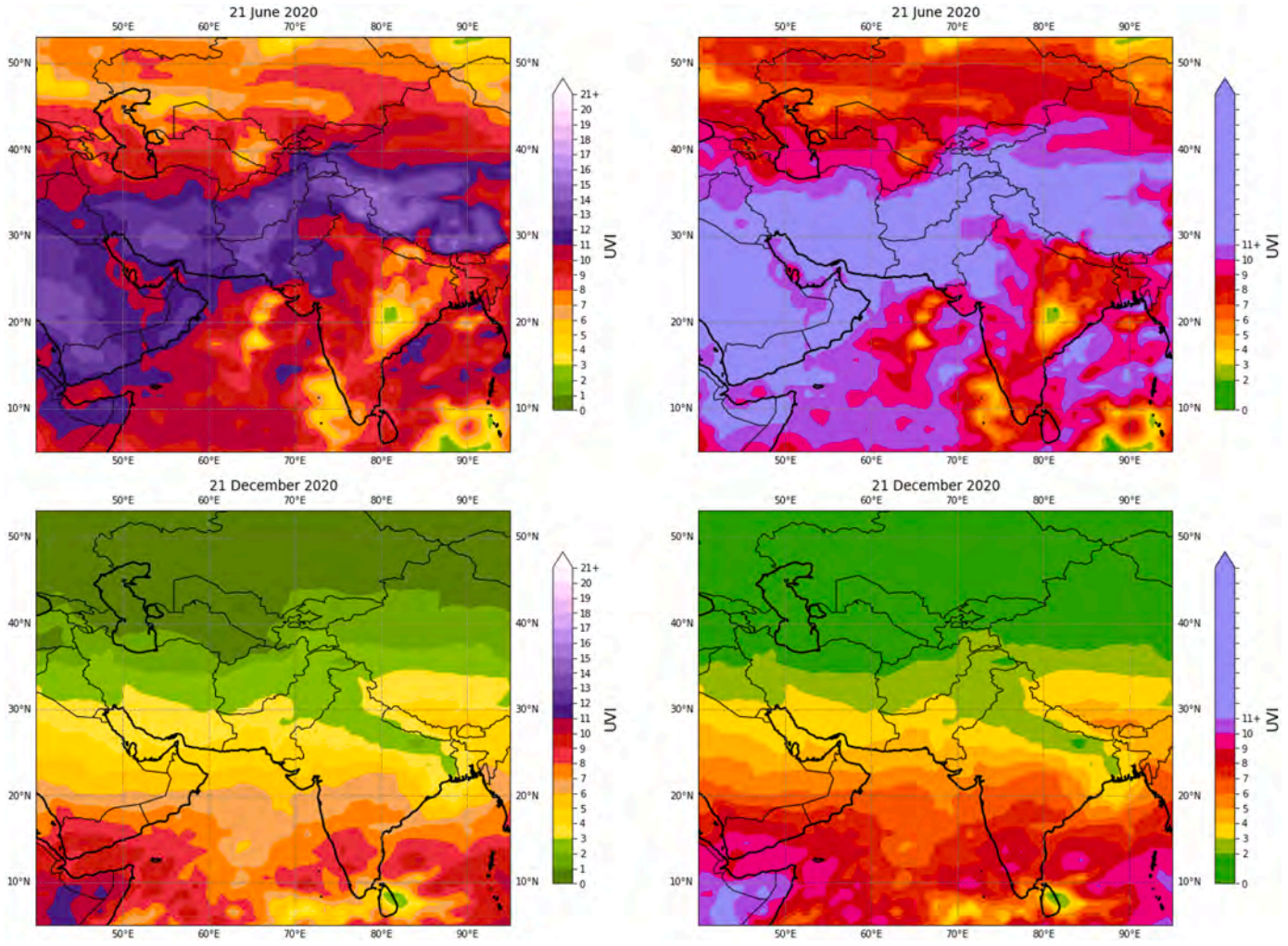

Fig. D2. Application of the proposed UCP_{UVI} (left) and comparison with the WHO [55] UCP_{UVI} (right) to a zoom on the maps of Fig. 3 spanning the highlands territory of the Tibet and its surroundings for 21 June 2020 (top) and 21 December 2020 (bottom).

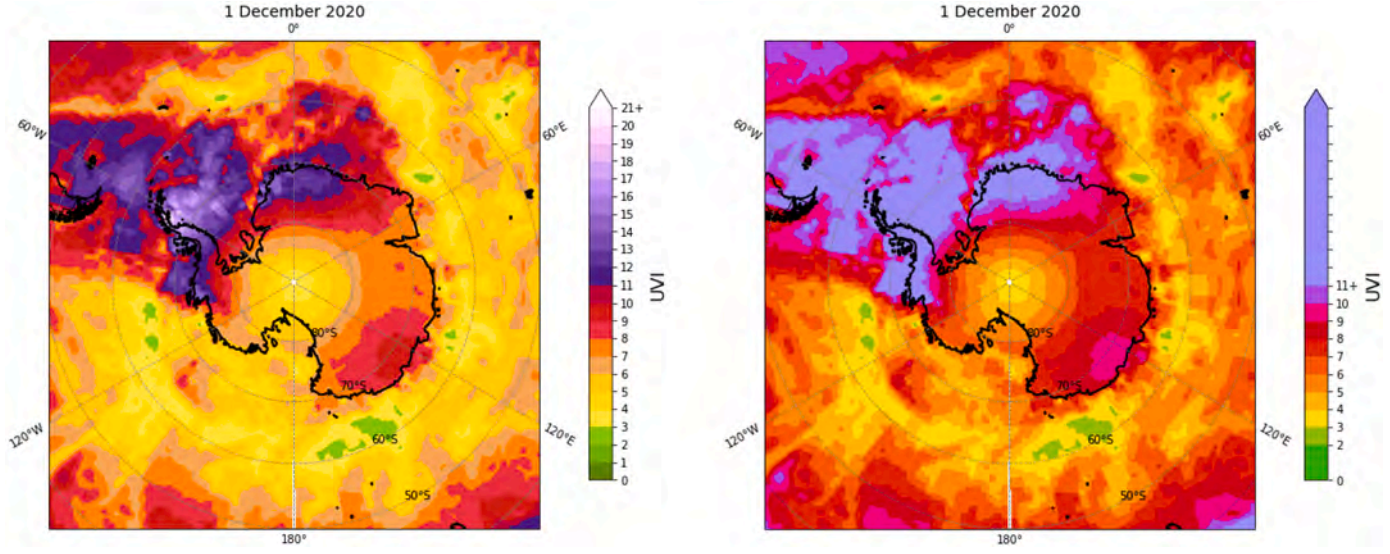

Fig. D3. Application of the proposed UCP_{UVI} (left) and comparison with the WHO [55] UCP_{UVI} (right) to an overpass event of the Antarctic ozone hole through continental areas of southern South America and its surroundings during day 01 December 2020. Noon all-sky UVI data provided by CERES (https://ceres.larc.nasa.gov/index.php).

References

[1] AGNIR (Advisory Group on Non-Ionizing Radiation). Health Effects from Ultraviolet Radiation. ed. R. Doll. UK National Radiological Protection Board, 13 (1), 2002.

[2] S. Allinson, M. Asmuss, C. Baldermann, J. Bentzen, D. Buller, N. Gerber, A. C. Green, R. Greinert, M. Kimlin, J. Kunrath, R. Matthes, L.C. Polzl-Viol, E. Rehfuess, C. Rossmann, N. Schuz, C. Sinclair, E. van Deventer, A. Webb, W. Weiss, G. Ziegelberger, Validity and use of the UV index: report from the UVI working group, Schloss Hohenkammer, Germany, 5-7 December 2011, Health Phys. 103 (3) (2012) 301–306, https://doi.org/10.1097/HP0b013e31825b581e.

[3] C. Alonso-Belmonte, T. Montero-Vilchez, S. Arias-Santiago, A. Buendía-Eisman, Current state of skin cancer prevention: a systematic review, ACTAS Dermo-Sifiliográficas 113 (8) (2022) T781–T791, https://doi.org/10.1016/j.ad.2022.04.018.

[4] P.W. Barnes, T.M. Robson, P.J. Neale, et al., Environmental effects of stratospheric ozone depletion, UV radiation, and interactions with climate change: UNEP environmental effects assessment panel, update 2021, Photochem. Photobiol. Sci. 21 (2022) 275–301, https://doi.org/10.1007/s43630-022-00176-5.

[5] L. Bartram, Abhisekh Patra, M. Stone, Affective color in visualization, in: Proceedings of the 2017 CHI Conference on Human Factors in Computing Systems, 2017, pp. 1364–1374, https://doi.org/10.1145/3025453.3026041.

[6] G.H. Bernhard, R.L. McKenzie, K. Lantz, et al., Updated analysis of data from palmer station, Antarctica (64° S), and San Diego, California (32° N), confirms large effect of the Antarctic ozone hole on UV radiation, Photochem. Photobiol. Sci. 21 (2022) 373–384, https://doi.org/10.1007/s43630-022-00178-3.

[7] M. Blumthaler, W. Ambach, R. Ellinger, Increase in solar UV radiation with altitude, J. Photochem. Photobiol. B: Biol. 39 (2) (1997) 130–134, https://doi.org/10.1016/S1011-1344(96)00018-8.

[8] M.M. Caldwell, L.O. Bjorn, J.F. Bornman, S.D. Flint, G. Kulandaivelu, A. H. Teramura, M. Tevini, Effects of increased solar ultraviolet radiation on terrestrial ecosystems, J. Photochem. Photobiol. B. 46 (1998) 40–52.

[9] N. Camgöz, C. Yener, D. Güvenç, Effects of hue, saturation, and brightness on preference, Color Res. Appl. 27 (3) (2002) 199–207, https://doi.org/10.1002/col.10051.

[10] A. Cede, E. Luccini, L. Nuñez, R.D. Piacentini, M. Blumthaler, Monitoring of erythemal irradiance in the Argentine ultraviolet network, J. Geophys. Res. 107 (D13) (2002) 4165, https://doi.org/10.1029/2001JD001206.

[11] Y. Chen, J. Yang, Q. Pan, M. Vazirian, S. Westland, A method for exploring word-colour associations, Color Res. Appl. 45 (2020) 85–94, https://doi.org/10.1002/col.22434.

[12] R.R. Cordero, A. Damiani, J. Jorquera, et al., Ultraviolet radiation in the Atacama desert, Antonie Van Leeuwenhoek 111 (2018) 1301–1313, https://doi.org/10.1007/s10482-018-1075-z.

[13] M. de Paula Corrêa, Solar ultraviolet radiation: properties, characteristics and amounts observed in Brazil and South America, An. Bras. Dermatol. 90 (3) (2015) 297–313, https://doi.org/10.1590/abd1806-4841.20154089.

[14] K. Diehl, T. Görig, C. Jansen, M.C. Hruby, A.B. Pfahlberg, O. Gefeller, I've heard of it, yes, but I can't remember what exactly it was" - a qualitative study on awareness, knowledge, and use of the UV index, Int. J. Environ. Res. Public Health. 18 (2021) 1615, https://doi.org/10.3390/ijerph18041615.

[15] B.L. Diffey, Solar ultraviolet radiation effects on biological systems, Phys. Med. Biol. 36 (3) (1991) 299–328, https://doi.org/10.1088/0031-9155/36/3/001. PMID: 1645473.

[16] O. Gefeller, S. Mathes, W. Uter, A.B. Pfahlberg, The role of the Global solar UV Index for sun protection of children in German kindergartens, Children 9 (2022) 198, https://doi.org/10.3390/children9020198.

[17] N. Gelsor, K. Ladislav, S. Jakob, T. Wangmu, P. Nima, Spatial distribution and temporal variation of solar UV radiation over the Tibetan Plateau, Appl. Phys. Res. 3 (2011).

[18] P. Gies, E. van Deventer, A.C. Green, C. Sinclair, R. Tinker, Review of the global solar UV index 2015, Workshop Report. Health Phys. 114 (1) (2018) 84–90, https://doi.org/10.1097/HP.0000000000000742.

[19] A.N. Gilbert, A.J. Fridlund, L.A. Lucchina, The color of emotion: a metric for implicit color associations, Food Qual. Prefer. 52 (2016) 203–210, https://doi.org/10.1016/j.foodqual.2016.04.007.

[20] A. Gjoni, Color coordination as a powerful design tool, Art and Design Rev. 10 (2022) 221–230, https://doi.org/10.4236/adr.2022.102016.

[21] A. Grzybowski, K. Kupidura-Majewski, What is color and how it is perceived? Clin. Dermatol. 37 (5) (2019) 392–401, https://doi.org/10.1016/j.clindermatol.2019.07.008.

[22] C.J. Heckman, K. Liang, M. Riley, Awareness, understanding, use, and impact of the UV index: a systematic review of over two decades of international research, Prev. Med. 123 (2019) 71–83, https://doi.org/10.1016/j.ypmed.2019.03.004.

[23] S.W. Hsiao, F.Y. Chiu, H.Y. Hsu, A computer-assisted colour selection system based on aesthetic measure for colour harmony and fuzzy logic theory, Color Res. Appl. 33 (2008) 411–423.

[24] IBM, NTSC luminance/chrominance equation definition for digital systems, in: IBM, 32, Tech. Discl., Bulletin, 1990, pp. 208–209.

[25] Intersun, in: WHO global UV project. 7th Intersun Meeting minutes. Portorož, Slovenia, 2018, 20 - 21 June, https://www.who.int/initiatives/intersun-programme.

[26] ISO / CIE (International Organization for Standardization / Commission Internationale de l'Eclairage), Joint ISO / CIE Standard: Erythema Reference Action Spectrum and Standard Erythema Dose. ISO 17166 / CIE S007 / E-1999, CIE Central Bureau, Vienna, Austria, 1999.

[27] N. Italia, E.A. Rehfuess, Is the Global Solar UV Index an effective instrument for promoting sun protection? A systematic review, Health Educ. Res. 27 (2012) 200–213.

[28] N. Kita, K. Miyata, Aesthetic rating and color suggestion for color palettes, Comput. Graphics Forum 35 (2016) 127–136, https://doi.org/10.1111/cgf.13010.

[29] M. Lambers, Interactive creation of perceptually uniform color maps, in: Proc. EuroVis Short Papers, 2020.

[30] C. Lara-Alvarez, T. Reyes, A geometric approach to harmonic color palette design, Color Res. Appl. 44 (2019) 106–114, https://doi.org/10.1002/col.22292.

[31] Lee-Taylor J., Madronich S., Fischer C., Mayer B. A climatology of UV radiation, 1979-2000, 65S-65N. In: Gao W., Slusser J.R., Schmoldt D.L. (eds) UV Radiation in Global Climate Change. Springer, Berlin, Heidelberg. 2010. 10.1007/978-3-642-03313-1_1.

[32] M. Lehmann, M. Heinitz, W. Uter, A. Pfahlberg, O. Gefeller, The extent of public awareness, understanding and use of the global solar UV index as a worldwide health promotion instrument to improve sun protection: protocol for a systematic review, BMJ Open 9 (2019), e028092, https://doi.org/10.1136/bmjopen-2018-028092 b.

[33] M. Lehmann, A.B. Pfahlberg, H. Sandmann, W. Uter, O. Gefeller, Public health messages associated with low UV Index values need reconsideration, Int. J. Environ. Res. Public Health 16 (2019) 2067, a.

[34] L. Lemus-Deschamps, L.S.Grainger Rikus, P.Sisson Gies, J, Li, Z. UV Index and UV dose distributions for Australia (1997-2001), Aus. Met. Mag. 53 (2004) 239–250.

[35] J.B. Liley, R.L. McKenzie, Where on Earth has the highest UV? in UV radiation and its effects: an update, RSNZ Miscellaneous Series, Dunedin 68 (2006) 36–37. https://www.niwa.co.nz/sites/default/files/import/attachments/Liley_2.pdf.

[36] H. Liu, B. Hu, L. Zhang, X.J. Zhao, K.Z. Shang, Y.S. Wang, J. Wang, Ultraviolet radiation over China: spatial distribution and trends, Renew. Sustain. Energy Rev. 76 (2017) 1371–1383. ISSN 1364-0321.

[37] H. Liu, B. Hu, L. Zhang, Y.S. Wang, P.F. Tian, Spatiotemporal characteristics of ultraviolet radiation in recent 54 years from measurements and reconstructions over the Tibetan Plateau, J. Geophys. Res. Atmos. 121 (2016) 7673–7690.

[38] Lucas R.M., Neale R.E., Madronich S., McKenzie R.L. Are current guidelines for sun protection optimal for health? Exploring the evidence. Photochem. Photobiol. Sci., 17, 1956–1963. 2018. doi: 10.1039/c7pp00374a. Correction: Photochem. Photobiol. Sci., 17, 1964-1964. 2018. doi: 10.1039/c8pp90034e.

[39] R.M. Lucas, S. Yazar, A.R. Young, M. Norval, F.R. De Gruijl, Y. Takizawa, L. E. Rhodes, C.A. Sinclair, R.E Neale, Human health in relation to exposure to solar ultraviolet radiation under changing stratospheric ozone and climate, Photochem. Photobiol. Sci. 18 (3) (2019) 641–680.

[40] E. Luccini, A. Cede, R. Piacentini, C. Villanueva, P. Canziani, Ultraviolet climatology over Argentina, J. Geophys. Res. 111 (2006) D17312, https://doi.org/10.1029/2005JD006580.

[41] R.L. McKenzie, R.M. Lucas, Reassessing impacts of extended daily exposure to low level solar UV radiation, Sci. Rep. 8 (2018) 13805, https://doi.org/10.1038/s41598-018-32056-3.

[42] J. McNames, An effective color scale for simultaneous color and gray-scale publications, IEEE Signal Process. Mag. 23 (1) (2006), https://doi.org/10.1109/MSP.2006.1593340.

[43] K. Moreland, Diverging color maps for scientific visualization, in: Proc. Int. Symp. Visual Computing, 2009.

[44] L.H.F. Mullenders, Solar UV damage to cellular DNA: from mechanisms to biological effects, Photochem. Photobiol. Sci. 17 (2018) 1842–1852, https://doi.org/10.1039/c8pp00182k.

[45] NASA Earth Observations. EOS Project Science Office. NASA Goddard Space Flight Center. 2011. https://neo.sci.gsfc.nasa.gov/view.php?datasetId=AURA_UVI_CLIM_M.

[46] R.E. Neale, R.M. Lucas, S.N. Byrne, et al., The effects of exposure to solar radiation on human health, Photochem. Photobiol. Sci. (2023), https://doi.org/10.1007/s43630-023-00375-8.

[47] P. Newman, R. McKenzie, UV impacts avoided by the Montreal Protocol, Photochem. Photobiol. Sci. 10 (2011) 1152–1160. https://pubs.rsc.org/en/content/articlelanding/2011/PP/c0pp00387e#!divAbstract.

[48] Newton I. Opticks, S. Smith and B. Walford. London, 1st edition, 1704 (available at, https://archive.org/details/1704-newton-opticks-1ed.

[49] F. Nollas, E. Luccini, G. Carbajal, F. Orte, E. Wolfram, G. Hülsen, J. Gröbner, Report of the Fifth Erythemal UV Radiometers Intercomparison (Buenos Aires, Argentina, GAW report, 2018, 2018.

[50] T.B. Plante, M Cushman, Choosing color palettes for scientific figures, Res. Pract. Thromb. Haemost. 4 (2020) 176–180, https://doi.org/10.1002/rth2.12308.

[51] W. Su, T.P. Charlock, F.G. Rose, Deriving surface ultraviolet radiation from CERES surface and atmospheric radiation budget: methodology, J. Geophys. Res. 110 (D14209) (2005), https://doi.org/10.1029/2005JD005794.

[52] H.-J. Suk, H Irtel, Emotional response to color across media, Color Res. Appl. 35 (2010) 64–77, https://doi.org/10.1002/col.20554.

[53] S.A. Umar, S.A. Tasduq, Ozone layer depletion and emerging public health concerns - an update on epidemiological perspective of the ambivalent effects of ultraviolet radiation exposure, Front. Oncol. 12 (2022), 866733, https://doi.org/10.3389/fonc.2022.866733.

[54] A.R. Webb, H. Slaper, P. Koepke, A.W. Schmalwieser, Know your standard: clarifying the CIE erythema action spectrum, Photochem. Photobiol. 87 (2011) 483–486, https://doi.org/10.1111/j.1751-1097.2010.00871.x.

[55] WHO (World Health Organization). Global solar UV index: a practical guide. A joint recommendation with the World meteorological organization, United Nations environment programme, and the international commission on non-ionizing radiation protection. 2002. https://apps.who.int/iris/handle/10665/42459.

[56] WHO news. SunSmart global UV App helps protect you from the dangers of the sun and promotes public health. 2022. https://www.who.int/news/item/21-06-2022-sunsmart-global-uv-app-helps-protect-you-from-the-dangers-of-the-sun-and-promotes-public-health.
[57] WHO. The UV index sun protection table. 2003. https://www.who.int/publications/m/item/the-uv-index-sun-protection-table.
[58] M. Wijffelaars, R. Vliegen, J.J. van Wijk, E.-.J. van der Linden, Generating color palettes using intuitive parameters, Comput. Graphics Forum 27 (3) (2008).
[59] L. Wilms, D. Oberfeld, Color and emotion: effects of hue, saturation, and brightness, Psychol. Res. 82 (2018) 896–914, https://doi.org/10.1007/s00426-017-0880-8.
[60] WMO (World Meteorological Organization), Executive summary. scientific assessment of ozone depletion: 2022, GAW Report 278 (2022) 56. WMO, Geneva, https://ozone.unep.org/system/files/documents/Scientific-Assessment-of-Ozone-Depletion-2022-Executive-Summary.pdf.
[61] J. Yang, Y. Chen, S. Westland, K Xiao, Predicting visual similarity between colour palettes, Color Res. Appl. 45 (2020) 401–408, https://doi.org/10.1002/col.22492.
[62] F. Zaratti, R. Piacentini, H. Guillén, S. Silva, J. Liley, R. McKenzie, Proposal for a modification of the UVI risk scale, Photochem. Photobiol. Sci. 13 (2014), https://doi.org/10.1039/c4pp00006d.